Necklace Globule and Counterion Condensation

Junhwan Jeon[†] and Andrey V. Dobrynin*[,‡]

Department of Chemical Engineering, Vanderbilt University, Nashville, Tennessee 37235, and
Department of Physics and Polymer Program, Institute of Materials Science, University of Connecticut,
Storrs, Connecticut 06269-3136

Received May 2, 2007; Revised Manuscript Received July 12, 2007

ABSTRACT: We have developed a necklace model of polyelectrolyte chain in which the necklace structure appears as a result of the counterion condensation on the polyelectrolyte backbone. This necklace structure optimizes the correlation-induced attraction of the condensed counterions and charged monomers and electrostatic repulsion between uncompensated charges. The new feature of this necklace globule is that it can be formed even in good solvent conditions for the polymer backbone. By using the scaling analysis, we have calculated the diagram of state of polyelectrolyte chain as a function of the solvent quality for the polymer backbone and value of the Bjerrum length. To test the predictions of a scaling model, we have performed molecular dynamics simulations of polyelectrolyte chains with the degrees of polymerizations $N = 124-304$ and fraction of charged monomers $f = {}^1/_3$ in good, θ, and poor solvent conditions for the polymer backbone. We have identified the range of parameters in which the necklace globule is formed due to correlation-induced attractive interactions in the good solvent conditions for the polymer backbone. The results of the molecular dynamics simulations are in qualitative agreement with the predictions of a scaling model.

1. Introduction

Polyelectrolytes are polymers with ionizable groups.[1−5] In polar solvents with high dielectric constants, these groups dissociate, leaving charged groups on the polymer backbone and releasing counterions into solution. The static and dynamics properties of polyelectrolyte solutions such as solution osmotic pressure, solution viscosity, chain's relaxation time, and diffusion coefficient strongly depend on the charge acquired by polyelectrolyte chains after dissociation process.[1−5] The amount of the ionized groups is very sensitive to the solution dielectric constant, solvent quality for the polymer backbone, and polymer and salt concentrations. For example, by decreasing a solution dielectric constant or by increasing the polymer or salt concentrations, one can reduce a net charge of a polyelectrolyte chain. This reduction of the polymeric charge is due to the counterion condensation on the polymer backbone.[2,3,6−9]

The idea of the counterion condensation was first introduced by Manning and Oosawa.[6−9] They have established that a charge of a rigid (rodlike) polyion depends on the fine interplay between the electrostatic attraction of a counterion to the polyelectrolyte backbone and configurational entropy loss due to counterion localization in the vicinity of the polymer chain. This theory showed that the linear charge density of a rodlike polyion cannot exceed a critical value that depends on the solution dielectric constant, temperature, and counterion valence determining the value of the Bjerrum length l_B. (The Bjerrum length $l_B = e^2/\epsilon k_B T$ is defined as the length scale at which the Coulomb interaction between two elementary charges e in a dielectric medium with the dielectric constant ϵ is equal to the thermal energy $k_B T$.)[6−9]

The situation is even more interesting in the case of flexible polyelectrolytes. In this case, a chain conformation is directly coupled with the intrachain electrostatic interactions that are controlled by the amount of the condensed counterions.[2,3,10−20] Thus, in addition to counterion configurational entropy and electrostatic interactions, the chain's conformational free energy comes into play. These contributing factors have to be optimized simultaneously to determine fraction of the condensed counterions and the equilibrium chain size. In the case of the good or θ solvents for the polymer backbone, the counterion condensation results in gradual decrease of the chain size with the increase of the polymer or salt concentrations.[3,10−12,21−23] A qualitatively different picture of counterion condensation is observed for polyelectrolytes in poor solvent conditions for the polymer backbone.[3,17,19,24] In a poor solvent, a polyelectrolyte chain forms a necklace globule of dense polymeric beads connected by strings of monomers.[17,19,25−40] The counterion condensation on the necklace globule can occur in avalanche-like fashion. By increasing polymer concentration or decreasing temperature, one can induce a spontaneous condensation of counterions inside beads of the necklace globule. This reduces the bead's charge and results in increase of the bead mass (size), which initiate further increase of the number of condensed counterions inside beads starting the avalanche-like counterion condensation process (see, for review, ref 3).

Note that, in addition to the reduction of the net polymeric charge weakening intrachain electrostatic repulsion, the condensed counterions can also induce effective attractive interactions between charged monomers.[11−13,16,23,26,41] In the ion binding and counterion adsorption models,[23,42,43] condensed counterions form ionic pairs with oppositely charged ions on the polymer backbone. The formation of the ionic pairs leads to an additional dipole−dipole and charge−dipole attractive interactions.[11,12,23] These attractive interactions decrease the value of the effective second virial coefficient for monomer−monomer interactions, shifting the position of the θ point. In the case of the strongly charged polyelectrolytes, the shift of the θ temperature could be significant and change the solvent quality for the polymer backbone to poor solvent conditions as the number of condensed counterions increases. This can result in a chain collapse and completely alter the scenario of the counterion condensation (see discussion above). The analysis

* Corresponding author.
[†] Vanderbilt University.
[‡] University of Connecticut.

10.1021/ma071005k CCC: $37.00

of the effect of the counterion condensation on conformations of a polyelectrolyte chain was done by Schiessel and Pincus,[11] and by Schiessel[12] in the framework of the scaling approach, and by Muthukumar[23] in the framework of the variational approach. These theories predict nonmonotonic dependence of the chain size on the solution dielectric constant ϵ and solution temperature T (solution Bjerrum length $l_B \sim 1/(\epsilon T)$). The chain size first increases with the increasing the value of the Bjerrum length then begins to decrease as the Bjerrum length exceeds the crossover value. This nonmonotonic dependence of the chain size is the manifestation of the 2-fold role of the electrostatic interactions. At low values of the Bjerrum length, the intrachain electrostatic repulsion controls the chain size. These interactions become stronger with increase of the value of the Bjerrum and force the polyelectrolyte chain to expand. At large values of the Bjerrum length, the condensed counterions reduce net polymeric charge, weakening the intrachain electrostatic repulsion, which together with the dipole−dipole and charge-dipole attractive interactions induce chain contraction.

However, computer simulations of polyelectrolyte solutions show that the condensed counterions are not permanently attached to oppositely charged groups on the polymer backbone as assumed by the ion-binding and ion adsorption models but rather localized near the polymer backbone and are free to move inside the chain volume.[13,21,26,27,41] The localization of counterions inside the chain volume can also lead to effective attractive interactions.[16,26] These interactions are due to heterogeneous distribution of the charge density along the polymer backbone. In the case of weak electrostatic attraction, the origin of these interactions is similar to the fluctuation-induced attraction in two-component plasma and is related to the local charge density fluctuations.[16] In the opposite limit of strong electrostatic interactions, the effect is due to correlation-induced attraction between the counterions and the oppositely charged polymer backbone similar to the interactions in strongly correlated Wigner liquids (see, for review, refs 44,45) or in ionic crystal such as NaCl. For example, in the case of the ionic crystal, the attractive (negative) lattice energy is due to the spatial distribution (spatial correlations) of cations and anions over the lattice sites even though the net charge of the crystal is zero. The crystal will remain stable even if it carries a small nonzero charge because of the large lattice (correlation) energy.

The effect of the fluctuation/correlation-induced attractive interactions on the conformations of a polyelectrolyte chain was studied theoretically[16,26] and by molecular dynamics simulations.[13,26,41] These studies show that the fluctuation/correlation-induced attractive interactions can cause additional chain collapse. In particular, in the case of the poor solvent conditions for the polymer backbone, these studies established the existence of the two different mechanisms that could lead to formation of the necklace globule.[26,30,41] For the values of the Bjerrum length $l_B = 1\sigma$ and 2σ, the necklace structure appears as a result of competition between short-range monomer−monomer attractive interactions and electrostatic repulsion between uncompensated charges.[41] However, for the value of the Bjerrum length $l_B = 3\sigma$, the necklace structure is controlled by counterion condensation and is due to the optimization of the correlation-induced attraction between charged monomers and condensed counterions and electrostatic repulsion between uncompensated charges on the polymer backbone.[26,41] It is important to point out that the short-range monomer−monomer attractions still play an important role in determining the crossover value of the Bjerrum length between two regimes. In the present paper, we extend the scaling analysis of the effect of the fluctuation/correlation-induced attractive interactions on chain conformations to the θ and good solvent regimes for the polymer backbone and study the stability of the necklace-like globule in this range of parameters. The rest of the manuscript is organized as follows. In Section 2, we show how the counterion condensation and correlation-induced-attraction modifies the diagram of state of a polyelectrolyte chain as a function of the fraction of the condensed counterions and solvent quality for the polymer backbone. The results of the scaling analysis are tested in Section 3, which provides an analysis of the simulation results for the chain size, fraction of the condensed counterions, and parameters of the necklace globule. Finally, in Section 4, we summarize our results.

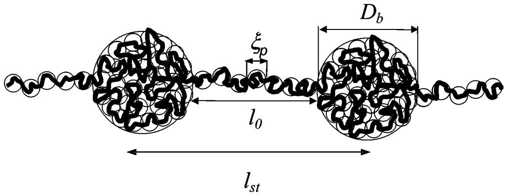

Figure 1. Schematic picture of a necklace formed by a polyelectrolyte chain.

2. Effect of Counterion Condensation on Necklace Globule

In this section, we will study the effect of the solvent quality for the polymer backbone and fraction of the condensed counterions on the chain's conformations. Consider a necklace-like polyelectrolyte chain with the degree of polymerization N, bond length b, and the fraction of charged monomers f. Let us assume that the necklace has n_b beads of size D_b with m_b monomers in each. These beads are connected by strings each having m_{str} monomers (see Figure 1). We will assume that the fraction x of counterions is condensed inside beads. The beads are globules with the monomer number density $\rho \approx m_b/D_b^3$. Because beads are charged globules, there are two different types of interactions inside a bead: short-range interactions between monomers and electrostatic interactions between charged monomers and counterions.

Each bead can be viewed as a droplet of semidilute polymer solution (see Figure 1) for which the contribution of the monomer−monomer repulsive interactions in the good solvent conditions for the polymer backbone to the bead free energy is[46−48]

$$\frac{F_b^{sh}}{k_B T} \approx m_b \tau^{3/4} (\rho b^3)^{5/4}, \text{ good solvent} \tag{1a}$$

where $\tau = 1 - \theta/T$ is the effective temperature and θ is the theta temperature, k_B is the Boltzmann constant, and T is the absolute temperature. In this section, the analysis of the necklace globule is done on the scaling level by neglecting all numerical coefficients.

In the case of the poor solvent conditions for the polymer backbone or in the case of the dense polymeric globules in which the two-body monomer−monomer repulsion is screened, the short-range interactions can be approximated by a virial expansion in the power series of monomer density ρ[46]

$$\frac{F_b^{sh}}{k_B T} \approx m_b b^3 \tau \rho + m_b b^6 \rho^2 \tag{1b}$$

Below the θ temperature that corresponds to the poor solvent conditions for the polymer backbone, the first term is negative. The crossover to concentrated solution regime inside the globule takes place at $\rho b^3 \approx |\tau|$. At higher polymer concentrations, $\rho b^3 \geq |\tau|$, the three-body monomer−monomer repulsion determines equilibrium density inside beads.

The electrostatic interactions inside a bead can be represented as a sum of the electrostatic repulsion between charged monomers (fm_b per bead), electrostatic attraction between charged monomers and condensed counterions (xfm_b per bead), and electrostatic repulsion between condensed counterions

$$\frac{U_{\text{electr}}}{k_BT} \approx \frac{l_B(fm_b)^2}{D_b} - 2\frac{l_Bx(fm_b)^2}{D_b} + \left\langle\frac{U_{\text{cc}}}{k_BT}\right\rangle_{\text{count}} \tag{2}$$

where the brackets $\langle\ \rangle_{\text{count}}$ denote averaging over distributions of counterions inside the bead. The Bjerrum length

$$l_B = e^2/(\epsilon k_BT) \tag{3}$$

determines the strength of the electrostatic interactions between two elementary charges e in the medium with the dielectric constant ϵ. In writing eq 2, we have assumed that the charged monomers are uniformly distributed over the bead volume. The eq 2 can be rewritten by adding and subtracting the electrostatic repulsion between condensed counterions uniformly distributed over the bead volume with average density $xf\rho$. After this transformation, the electrostatic energy of a bead has the following form

$$\frac{U_{\text{electr}}}{k_BT} \approx \frac{l_B[(1-x)fm_b]^2}{D_b} + \left\langle\frac{U_{\text{cc}}}{k_BT}\right\rangle_{\text{count}} - \frac{l_B(xfm_b)^2}{D_b} \tag{4}$$

The first term describes the electrostatic repulsion of the uniformly charged bead with the effective charge $(1-x)fm_b$. The last two terms in the eq 4 represent electrostatic interactions between condensed counterions and oppositely charged neutralizing background with charge density $xf\rho$. This part of the bead electrostatic energy is known as the correlation part of the one-component plasma (OCP) free energy (see, for details, refs 16,44,45). The averaging of electrostatic interactions between condensed counterions and neutralizing background results in an additional correlation-induced attractive contribution to the bead electrostatic energy.

In a globule with polymer density ρ, condensed counterions are separated by a typical distance

$$\xi_c \approx (xf\rho)^{-1/3} \tag{5}$$

The correlation-induced attraction between counterions can be estimated as an electrostatic attraction of a counterion and the oppositely charged neutralizing background with the effective charge density $xf\rho$ inside radius ξ_c. This leads to the correlation-induced attraction to be on the order of

$$\varphi_{\text{cor}} \approx -k_BTl_B/\xi_c \tag{6}$$

per condensed counterion. In the above estimate of the correlation-induced attraction, we used the strong correlation approximation for the OCP in which the interaction parameter l_B/ξ_c is large, $l_B/\xi_c \geq 1$. In the case of weak interactions, $l_B/\xi_c \ll 1$, the attraction energy between a counterion and neutralizing background has a well-known Debye−Huckel form[16,45]

$$\varphi_{\text{cor}} \approx -k_BT(l_B/\xi_c)^{3/2} \tag{7}$$

The correlation-induced attractive interaction energy between counterions and neutralizing background in a bead is equal to

$$\frac{U_{\text{OCP}}}{k_BT} \approx \left\langle\frac{U_{\text{cc}}}{k_BT}\right\rangle - \frac{l_B(xfm_b)^2}{D_b} \approx \frac{m_bxf\varphi_{\text{cor}}}{k_BT} \approx -m_bxf \begin{cases} l_B/\xi_c, & \text{for } \xi_c \leq l_B \\ (l_B/\xi_c)^{3/2}, & \text{for } \xi_c \gg l_B \end{cases} \tag{8}$$

The total electrostatic energy of a bead with condensed counterions is the sum of the repulsive and attractive terms

$$\frac{F_b^{\text{elec}}}{k_BT} \approx \frac{l_B[(1-x)fm_b]^2}{D_b} + m_bxf\frac{\varphi_{\text{cor}}}{k_BT} \tag{9}$$

2.1. Necklace Globule in a Good Solvent. We begin our discussion by considering the possibility of the necklace formation in good solvent conditions for the polymer backbone. The total bulk energy of all beads in good solvent conditions for the polymer backbone is equal to the sum of the short-range (eq 1a) and electrostatic (eq 9) energies times the number of beads per chain n_b. In the limit when the most of the polymeric mass is stored inside beads, $m_b/m_{\text{str}} \gg 1$, the number of beads per chain can be estimated as $n_b \approx N/m_b$.

$$\frac{F_{\text{bulk}}}{k_BT} \approx N\frac{l_B[(1-x)f]^2m_b}{D_b} + N(\tau^{3/4}(b^3\rho)^{5/4} + xf\varphi_{\text{cor}}/k_BT) \tag{10}$$

It is important to point out that, in this approximation, $m_b/m_{\text{str}} \gg 1$, the total free energy of the necklace splits into independent contributions from beads and strings. Thus, the equilibrium necklace parameters can be found separately minimizing the bead's and string's contributions to the necklace free energy (see, for review, ref 3). Note that the first term on the right-hand side of the eq 10 is on the order of the bead surface energy and can be neglected during the bead density optimization (see eq 17 below). The equilibrium polymer density inside a bead is obtained by minimizing the terms in the parenthesis on the right-hand side of eq 10 with respect to the polymer density ρ. This results in the following expression for the polymer density inside a bead

$$\rho b^3 \approx \begin{cases} u^{12/11}(xf)^{16/11}/\tau^{9/11}, & \text{strongly correlated} \\ (uxf)^2/\tau, & \text{weakly correlated} \end{cases} \tag{11}$$

where u is the ratio of the Bjerrum length l_B to the bond size b, $u = l_B/b$. The first regime in eq 11 corresponds to the case of strong correlations between condensed counterions with interaction parameter, $l_B/\xi_c \geq 1$. Note that the monomer density in eq 11 is inversely proportional to the effective temperature τ, indicating that it will decrease with increasing the strength of the monomer−monomer repulsion.

The polymer density fluctuations inside the bead with polymer density ρ given by eq 11 occur at the length scales smaller than the correlation length ξ_p. At these length scales, the chain conformations are unperturbed by the polymer−counterion attractive interactions and are those of a chain of g_p monomers in a good solvent ($\xi_p \approx b\tau^{1/5}g_p^{3/5}$).[46,48] At the length scales larger than the correlation blob size ξ_p, the density fluctuations are suppressed and correlation blobs in a bead are densely packed, $\rho \approx g_p/\xi_p^3$. The number of monomers in a correlation blob is equal to

$$g_{\mathrm{p}} \approx \begin{cases} \tau^{3/11} u^{-15/11} (xf)^{-20/11}, & \text{strongly correlated} \\ \tau^{1/2} (uxf)^{-5/2}, & \text{weakly correlated} \end{cases} \qquad (12)$$

and its size is

$$\xi_{\mathrm{p}} \approx b \begin{cases} \tau^{4/11} u^{-9/11} (xf)^{-12/11}, & \text{strongly correlated} \\ \tau^{1/2} (uxf)^{-3/2}, & \text{weakly correlated} \end{cases} \qquad (13)$$

The polymeric correlation length ξ_{p} in the case of the weakly correlated condensed counterions is on the order of the Debye screening length r_{D} due to condensed counterions $\xi_{\mathrm{p}} \approx r_{\mathrm{D}} \approx (l_{\mathrm{b}} x f \rho)^{-1/2} \approx b\tau^{1/2}(uxf)^{-3/2}$ (see eq 13), and both charge and polymer density fluctuations occur on the same length scale. Note that, in the case of strongly correlated counterions, the correlation blob size ξ_{p} is smaller than the average distance between condensed counterions ξ_{c}.

The bulk free energy of all beads with equilibrium density ρ is on the order of

$$\frac{F_{\mathrm{bulk}}}{k_{\mathrm{B}}T} \approx N \frac{l_{\mathrm{B}}[(1-x)f]^2 g_{\mathrm{p}}^{1/3}}{\xi_{\mathrm{p}}} m_{\mathrm{b}}^{2/3} - N/g_{\mathrm{p}} \qquad (14)$$

where we use the following relation between the bead size D_{b} and the number of monomers in it, $D_{\mathrm{b}} \approx \xi_{\mathrm{p}}(m_{\mathrm{b}}/g_{\mathrm{p}})^{1/3}$. The last term on the right-hand side of eq 16 can be considered as the number of monomers in a chain times the chemical potential of a monomer inside the bead. This term represents the effective correlation-induced attractive interactions between monomers that are on the order of the thermal energy $k_{\mathrm{B}}T$ per each polymeric correlation blob inside the bead.

For the dense polymeric bead, there is also a surface energy contribution to the bulk free energy.[46,48] The origin of the surface energy is the difference in the number of the nearest neighbors for the condensed counterions at the surface of the bead and for the counterions inside the bead. In the case of the strongly correlated counterion system, the surface energy of a bead is estimated as the number of condensed counterions at the bead surface $(D_{\mathrm{b}}/\xi_{\mathrm{c}})^2$ times the energy of electrostatic interaction between a counterion and its neutralizing background $k_{\mathrm{B}}Tl_{\mathrm{B}}/\xi_{\mathrm{c}}$

$$F_{\mathrm{surf}} \approx k_{\mathrm{B}}T \frac{D_{\mathrm{b}}^2 l_{\mathrm{B}}}{\xi_{\mathrm{c}}^3} \approx k_{\mathrm{B}}T \frac{l_{\mathrm{B}} x f g_{\mathrm{p}}^{1/3}}{\xi_{\mathrm{p}}} m_{\mathrm{b}}^{2/3} \approx k_{\mathrm{B}}T\gamma m_{\mathrm{b}}^{2/3}$$

where γ is the dimensionless parameter, which is defined below. The surface energy of a bead in the weakly correlated case is $k_{\mathrm{B}}T$ per correlation blob of size ξ_{p} at the surface of the bead. There are $(m_{\mathrm{p}}/g_{\mathrm{p}})^{2/3}$ such blobs per bead. Taking this into account, the surface energy term is

$$F_{\mathrm{surf}} \approx k_{\mathrm{B}}T \left(\frac{m_{\mathrm{b}}}{g_{\mathrm{p}}}\right)^{2/3} \approx k_{\mathrm{B}}T\gamma m_{\mathrm{b}}^{2/3}$$

Thus, surface free energy in both strongly correlated and weakly correlated cases is written in the same form

$$F_{\mathrm{surf}} \approx k_{\mathrm{B}}T\gamma m_{\mathrm{b}}^{2/3} \qquad (15)$$

where the dimensionless parameter

$$\gamma \approx \begin{cases} \tau^{-3/11} u^{15/11} (xf)^{49/33}, & \text{strongly correlated} \\ \tau^{-1/3} (uxf)^{5/3}, & \text{weakly correlated} \end{cases} \qquad (16)$$

The total contribution to the necklace free energy includes the surface energy contribution from all beads and bulk free energy contribution given by eq 14. Taking this into account, we can write the total bead free energy as

$$\frac{F_{\mathrm{bead}}}{k_{\mathrm{B}}T} \approx N\left(\frac{\gamma}{m_{\mathrm{b}}^{1/3}} + \frac{l_{\mathrm{B}}[(1-x)f]^2 g_{\mathrm{p}}^{1/3}}{\xi_{\mathrm{p}}} m_{\mathrm{b}}^{2/3} - g_{\mathrm{p}}^{-1}\right) \qquad (17)$$

Because this part of the necklace free energy depends only on the number of monomers in a bead m_{b}, the equilibrium number of monomers in a bead, $m_{\mathrm{b},}^*$ is obtained by minimizing the electrostatic and surface energies of the beads with respect to m_{b}

$$m_{\mathrm{b}}^* \approx \frac{x}{(1-x)^2 f} \qquad (18)$$

The dependence of the number of monomers in a bead on the fraction of condensed counterions x has the same form in both weakly and strongly correlated limits. The number of monomers in a bead increases as the fraction of the condensed counterions x increases.

The beads are connected by strings of monomers (see Figure 1). The equilibrium string length l_0 and the number of monomers per string m_{str} can be estimated by balancing the energy of the electrostatic repulsion between two neighboring beads and the free energy of a string. Pulling monomers into a string requires extra energy $k_{\mathrm{B}}T/g_{\mathrm{p}}$ per monomer that is the difference between the average interaction energy of a monomer in a string and that in the interior (or even at the surface) of a bead. Thus, each string has an additional positive contribution to the necklace free energy due to the loss of favorable attractive interactions between charged monomers and condensed counterions.

$$\frac{F_{\mathrm{str}}^{\mathrm{surf}}}{k_{\mathrm{B}}T} \approx m_{\mathrm{str}}/g_{\mathrm{p}} \qquad (19)$$

In addition to the surface free energy term, there is also an elastic contribution to the free energy of a string due to the stretching of polymer backbone between beads. Combining elastic and surface free energy contributions, we can write a string free energy as

$$\frac{F_{\mathrm{str}}}{k_{\mathrm{B}}T} \approx \left(\frac{l_0^2}{b^2 m_{\mathrm{str}}} + \frac{m_{\mathrm{str}}}{g_{\mathrm{p}}}\right) \qquad (20)$$

where l_0 is the length of a strand with m_{str} monomers between beads (see Figure 1). Minimization of the eq 20 with respect to the number of monomers in a string, m_{str}, at fixed length of a strand l_0 results in the relation connecting the distance between two neighboring beads and the number of monomers in a string m_{str}.

$$m_{\mathrm{str}} \approx g_{\mathrm{p}}^{1/2} \frac{l_0}{b} \qquad (21)$$

Substitution of eq 21 into eq 20 leads to the linear dependence of the string's free energy on its length l_0

$$\frac{F_{\mathrm{str}}}{k_{\mathrm{B}}T} \approx \frac{l_0}{g_{\mathrm{p}}^{1/2} b} \qquad (22)$$

The equilibrium length of a string is estimated by balancing the sum of the electrostatic repulsion between two neighboring beads and string free energy

$$\frac{F}{k_BT} \approx \frac{l_B[(1-x)fm_b^*]^2}{l_{str}} + \frac{l_0}{bg_p^{1/2}} \tag{23}$$

where l_{str} is the distance between center of mass of two neighboring beads, $l_{str} = D_b + l_0$, which in the limit of long strings is reduced to $l_{str} \approx l_0$. Minimization of eq 23 with respect to l_{str} results in

$$l_{str} \approx bg_p^{1/4}u^{1/2}(1-x)fm_b^* \approx b\frac{x}{1-x}\begin{cases}\tau^{3/44}u^{7/44}(xf)^{-5/11}, & \text{strongly correlated}\\ \tau^{1/8}u^{-1/8}(xf)^{-5/8}, & \text{weakly correlated}\end{cases} \tag{24}$$

In the case of the large beads, when the number of monomers in a bead is much larger than the number of monomers in a string, $m_b/m_{str} \gg 1$, the number of beads n_b per chain is approximately equal to N/m_b. Because most of the length of the necklace is stored in the strings, this necklace length can be estimated as the number of strings $n_b - 1$ on the chain times the distance between the centers of mass of two neighboring beads l_{str}

$$R_e \approx (n_b - 1)l_{str} \approx b(1-x)fN\begin{cases}\tau^{3/44}u^{7/44}(xf)^{-5/11}, & \text{strongly correlated}\\ \tau^{1/8}u^{-1/8}(xf)^{-5/8}, & \text{weakly correlated}\end{cases} \tag{25}$$

It follows from eq 25 that the necklace size decreases with increasing the fraction of the condensed counterions x. This is due to the fact that, with increasing the fraction of the condensed counterions, the bead size increases while their number per chain decreases.

To obtain total free energy of the necklace globule in a good solvent for the polymer backbone, we have to combine contributions from electrostatic and monomer−monomer interactions and surface energy contribution. The total free energy of the necklace has the following form

$$\frac{F_{neck}}{k_BT} \approx N\left(\frac{l_B(1-x)^{2/3}x^{2/3}f^{4/3}g_p^{1/3}}{\xi_p} - g_p^{-1}\right) \tag{26}$$

In writing the last equation, we have assumed that the most of the necklace mass is stored inside beads, $m_b/m_{str} \gg 1$.

Figure 2 shows the diagram of the different collapse mechanisms of the polymeric beads (chain) in the effective temperature τ and fraction of the condensed counterions xf plane. At small fractions of the condensed counterions (regime I), the correlation-induced attractive interactions are too weak to force a chain collapse. In this regime, a chain keeps its good solvent configuration. The crossover to the weakly correlated regime occurs when there is more than one correlation blob per chain, $g_p < N$, or $\tau \leq N^2(uxf)^5$. It is important to point out that the two-body monomer−monomer repulsive interactions are strong enough to swell a polymer chain only when the effective temperature τ is larger than $N^{-1/2}$. The line $\tau \sim N^{-1/2}$ represents the low boundary for the good solvent regime I. In the regime II, the chain is collapsed. In this regime, the equilibrium density inside beads is determined by balancing the two-body monomer−monomer repulsion and correlation-induced attraction. We subdivided this regime into IIa and IIb regimes to separate between weakly and strongly correlated cases. The low boundary of this regime is given by the following equation

$$\tau \approx \begin{cases}u^{3/5}(xf)^{4/5}, & \text{strongly correlated}\\ uxf, & \text{weakly correlated}\end{cases} \tag{27}$$

These two lines represent the crossover to concentrated solution regime inside collapsed beads, $\rho b^3 \approx \tau$.

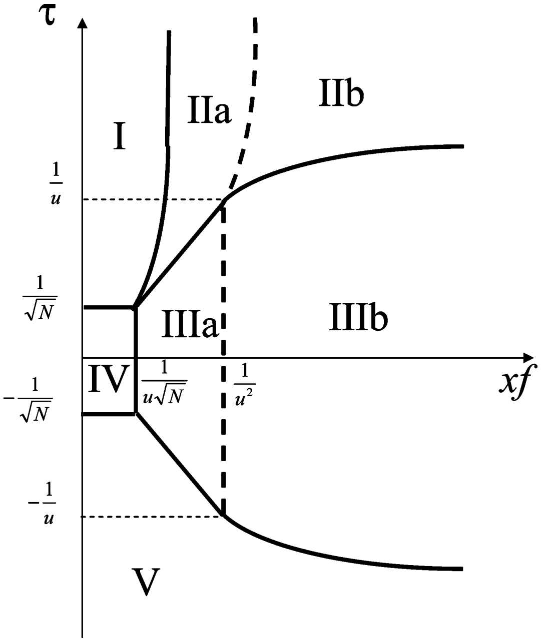

Figure 2. Diagram of different collapse mechanisms. Regime I: swollen chain in a good solvent. Regime II: chain collapse is due to correlation-induced attraction between condensed counterions and charged monomers. The equilibrium density inside beads is stabilized by two-body monomer−monomer repulsion. Regime III: equilibrium density inside beads is stabilized by three-body monomer−monomer repulsion. Regime IV: θ-solvent regime for the polymer backbone. Regime V: chain collapse is due to two-body monomer−monomer attraction (poor solvent conditions for the polymer backbone). Regimes a and b refer to weakly and strongly correlated cases.

Thus, we have shown that it is possible to form a necklace-like globule even in the case of the good solvent. In this case, the formation of the necklace globule is driven exclusively by a counterion condensation.

2.2. Necklace Structure Stabilized by Three-Body Repulsion. In the case of the dense polymeric globules, the three-body monomer−monomer repulsion play a dominant role in determining the equilibrium density inside the beads. This regime is shown in Figure 2 as regimes IIIa and IIIb. The bead's bulk free energy in this regime is written as follows

$$\frac{F_{bulk}}{k_BT} \approx N\frac{l_B[(1-x)f]^2m_b}{D_b} + N(b^6\rho^2 + xf\varphi_{cor}/k_BT) \tag{28}$$

The equilibrium polymer density inside a bead is obtained by minimizing the terms in the parenthesis on the right-hand side of eq 28 with respect to the polymer density ρ. This results in the following expression for the polymer density inside a bead

$$\rho b^3 \approx \begin{cases}u^{3/5}(xf)^{4/5}, & \text{strongly correlated}\\ uxf, & \text{weakly correlated}\end{cases} \tag{29}$$

Once again, we can use the correlation blob picture to describe the polymer density fluctuations inside beads with polymer density ρ. In the case when the three-body interactions play a

Table 1. Parameters of the Necklace Globule in Different Regimes

	good solvent		three-body		
	WC	SC	WC	SC	poor solvent
ρb^3	$(uxf)^2/\tau$	$u^{12/11}(xf)^{16/11}/\tau^{9/11}$	uxf	$u^{3/5}(xf)^{4/5}$	$\lvert\tau\rvert$
ξ_p/b	$\tau^{1/2}(uxf)^{-3/2}$	$\tau^{4/11}u^{-9/11}(xf)^{-12/11}$	$(uxf)^{-1}$	$u^{-3/5}(xf)^{-4/5}$	$\lvert\tau\rvert^{-1}$
g_p	$\tau^{1/2}(uxf)^{-5/2}$	$\tau^{3/11}u^{-15/11}(xf)^{-20/11}$	$(uxf)^{-2}$	$u^{-6/5}(xf)^{-8/5}$	$\lvert\tau\rvert^{-2}$
m_b	$xf/\Delta f^2$	$xf/\Delta f^2$	$xf/\Delta f^2$	$xf/\Delta f^2$	$\lvert\tau\rvert/(u\Delta f^2)$
D_b/b	$\tau^{1/3}u^{-2/3}(xf)^{-1/3}\Delta f^{-2/3}$	$\tau^{3/11}u^{-4/11}(xf)^{-5/33}\Delta f^{-2/3}$	$(u\Delta f^2)^{-1/3}$	$u^{-1/5}(xf)^{1/15}\Delta f^{-2/3}$	$(u\Delta f^2)^{-1/3}$
l_{str}/b	$\tau^{1/8}u^{-1/8}(xf)^{3/8}/\Delta f$	$\tau^{3/44}u^{7/44}(xf)^{6/11}/\Delta f$	$(xf)^{1/2}/\Delta f$	$u^{1/5}(xf)^{3/5}/\Delta f$	$\lvert\tau\rvert^{1/2}u^{-1/2}/\Delta f$
R_e/b	$\tau^{1/8}u^{-1/8}(xf)^{-5/8}\Delta fN$	$\tau^{3/44}u^{7/44}(xf)^{-5/11}\Delta fN$	$(xf)^{-1/2}\Delta fN$	$u^{1/5}(xf)^{-2/5}\Delta fN$	$u^{1/2}\lvert\tau\rvert^{-1/2}\Delta fN$

where we introduced $\Delta f=(1\text{-}x)f$.

dominant role, conformations of a chain section inside the correlation blob ξ_p are those of an ideal chain of g_p monomers ($\xi_p \approx bg_p^{1/2}$). This results in the number of monomers in a correlation blob to be given by

$$g_p \approx \begin{cases} u^{-6/5}(xf)^{-8/5}, & \text{strongly correlated} \\ (uxf)^{-2}, & \text{weakly correlated} \end{cases} \tag{30}$$

and correlation blob size to be equal to

$$\xi_p \approx b\begin{cases} u^{-3/5}(xf)^{-4/5}, & \text{strongly correlated} \\ (uxf)^{-1}, & \text{weakly correlated} \end{cases} \tag{31}$$

The analysis of the necklace structure in this range of parameters is similar to one presented in Section 2.1 and was discussed in detail by Liao et al. (see ref 26). The final results for the equilibrium number of monomers in a bead, the bead free energy, string length, size of the necklace globule, and the necklace free energy can be obtained by substituting expressions for the number of monomers in the correlation blob and its size, eqs 30 and 31, into eqs 14−26. The calculations are straightforward and we will not discuss them here. The final results are summarized in Table 1. It is important to point out that this analysis leads to the equilibrium number of monomers per bead m_b^* to be given by eq 18. Thus, the number of monomers in a bead has the same form independent of the form of terms describing the monomer−monomer repulsive interactions when the chain collapse is controlled by the counterion condensation inside beads.

In regime IV, the correlation-induced attractive interactions are weak and a chain keeps its Gaussian configuration. The boundary between regimes IV and IIIa is determined by the condition $g_p \sim N$, $xf \approx u^{-1}N^{-1/2}$.

2.3. Necklace Formation in a Poor Solvent. In the poor solvent conditions for the polymer backbone, we have to include two-body monomer−monomer attractive interactions into the bead's bulk free energy

$$\frac{F_{bulk}}{k_BT} \approx N\frac{l_B[(1-x)f]^2 m_b}{D_b} + N(\tau b^3\rho + b^6\rho^2 + xf\varphi_{cor}/k_BT) \tag{32}$$

The equilibrium polymer density inside a bead is obtained by minimizing the terms in the parenthesis on the right-hand side of eq 32 with respect to polymer density ρ. The balance of the first two terms in the parentheses results in the classical expression for the density inside a polymeric globule, $\rho \approx b^{-3}|\tau|$. In this case, the bead collapse is induced by the two-body attractive interactions. However, in the case when the correlation-induced attractive interactions are stronger than the two-body monomer−monomer attraction, the equilibrium density inside a bead is determined by the balance of the second and the third terms in the parentheses on the right-hand side of eq 32. This regime is similar to the regime considered in Section 2.2.

By analyzing terms on the right-hand side of the eq 32 and using the expressions for the equilibrium polymer density inside a bead eq 29, one can establish that the correlation-induced attraction dominates over the two-body attraction if the effective temperature $\tau > -u^{3/5}(xf)^{4/5}$ for the range of parameters $l_B/\xi_c \gg 1$ (see Figure 2, regime IIIb). The second regime in eq 29 corresponds to weakly correlated condensed counterions, $l_B/\xi_c \ll 1$. The boundaries of this regime IIIa are $xf \approx u^{-2}$ and $\tau \approx -uxf$, where the first condition determines the crossover between weakly and strongly correlated regimes ($\xi_c \approx l_B$), and the second boundary condition corresponds to crossover to the regime in which the globule is collapsed by the two-body attraction (see Figure 2). Outside of this envelope of parameters, the equilibrium polymer density inside the bead is determined by balancing two- and three-body interactions (see eq 32) (regime V in Figure 2). This leads to the necklace structure obtained by Dobrynin, Obukhov, and Rubinstein.[25] In this case, the optimal bead size is given by the following equation

$$m_b^* \approx \frac{|\tau|}{uf^2(1-x)^2}, \quad \text{solvophobic interactions} \tag{33}$$

Other characteristics of the necklace globule in this regime (regime V) are listed in Table 1.

Equations 33 and 18 give simple relations between the optimal number of monomers in a bead and the fraction of condensed counterions, x. Thus, by changing the value of the Bjerrum length l_B and the strength of the short-range interactions, one can explore different collapse regimes of the necklace-like globule.

2.4. Diagram of State of a Polyelectrolyte Chain. In this section, we present a diagram of state of a polyelectrolyte chain as a function of the effective fraction of charged monomers $\Delta f = (1 - x)f$ and the fraction of condensed counterions fx corresponding to positive range of the effective temperatures $\tau > 1/u$. There are four different regions in the diagram of states. In regime I, both electrostatic repulsion between uncompensated charges and correlation-induced attraction between condensed counterions are too weak to perturb chain conformations. At the upper boundary for this regime, the chain degree of polymerization N is on the order of the number of monomers in the electrostatic blob in the good solvent conditions for the polymer backbone, $g_e \approx \tau^{1/7}(u\Delta f^2)^{-2/7}$.[3,49] At the right vertical boundary of this regime, the chain degree of polymerization N is on the order of the number of monomers in the polymeric correlation blob g_p. For the larger fraction of the condensed counterions, the correlation-induced attractions cause chain

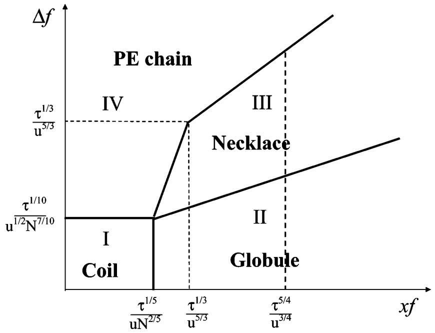

Figure 3. Diagram of states of a polyelectrolyte chain in a dilute solution in the parameter space of the fraction of the condensed counterions xf and the effective fraction of ionized groups $\Delta f = (1 - x)f$ (logarithmic scales). Regime I: coil-like chain. Regime II: collapsed polymeric globule. Regime III: necklace-like chain of the dense beads connected by narrow strings. Regime IV: polyelectrolyte chain regime. The vertical dashed lines in the regimes II and III separate regimes with different collapse mechanisms.

collapse. In this interval of parameters, a polyelectrolyte chain forms a spherical globule (regime II). The upper boundary for this regime is given by $\Delta f \approx (xf/N)^{1/2}$ and is obtained from the Rayleigh stability condition eq 18 by substituting N for the number of monomers in a bead. In the case of a small fraction of condensed counterions, xf, the polyelectrolyte chain forms a necklace globule with large beads and long strings (regime III). The increase of the effective fraction of charged monomers Δf in this regime leads to the decrease of the bead size and at the same time to the decrease in the length of the string connecting beads. The size of beads decreases, and thus the number of beads per chain increases with increasing Δf.

In the case of weakly interacting counterions, $xf < \tau^{1/3}u^{-5/3}$, the bead size becomes comparable with the polymeric correlation length ξ_p at $\Delta f \approx \tau^{-1/4}u^{5/4}(xf)^{7/4}$. Along this line, the bead's size is on the order of the string thickness, leading to the uniform distribution of polymeric mass along the chain end-to-end distance. At higher values of the effective fraction Δf of charged monomers, the chain conformation is that of an array of electrostatic blobs with size $D_e \approx \tau^{2/7}(u\Delta f^2)^{-3/7}$. In the strongly correlated case, there is one condensed counterion per each bead when the bead size D_b becomes comparable with the distance between condensed counterions ξ_c for $xf > \tau^{1/3}u^{-5/3}$. This takes place along the line $\Delta f \approx xf$. In Figure 3, we refer to this regime as regime IV (PE chain).

In the next section, we use molecular dynamics simulations to study different conformation regimes of a polyelectrolyte chain as a function of the Bjerrum length and the solvent quality for the polymer backbone.

3. Molecular Dynamics Simulations of the Counterion Condensation Induced Chain Collapse

3.1. Simulation Details. To test the predictions of the scaling model, we performed molecular dynamics simulations of a single polyelectrolyte chain with explicit counterions. A chain was modeled by a chain of charged Lennard-Jones particles with diameter σ and consisting of $N = 124$, 187, 244, and 304 particles. Every third particle on the polyelectrolyte chain was carrying a negative elementary charge, $-e$. This corresponds to the fraction of charged monomers, f, on the polymer backbone to be equal to $f = 1/3$.

The connectivity of particles into polymer chains was maintained by the finite extension nonlinear elastic (FENE) potential,[50]

$$U_{\mathrm{FENE}}(r) = -0.5k_{\mathrm{spring}}R_{\mathrm{max}}^2 \ln\left(1 - \frac{r^2}{R_{\mathrm{max}}^2}\right) \tag{34}$$

where k_{spring} is the spring constant set to be $k_{\mathrm{spring}} = 7k_BT/\sigma^2$ and the maximum bond length is $R_{\mathrm{max}} = 2\sigma$, k_B is the Boltzmann constant, and T is the absolute temperature.

Electrostatic interactions between any two charged particles with charge valences q_i and q_j, and separated by a distance r_{ij}, was given by the Coulomb potential,

$$U_{\mathrm{Coul}}(r_{ij}) = k_BT\frac{l_Bq_iq_j}{r_{ij}} \tag{35}$$

The strength of the electrostatic interactions is determined by the value of the Bjerrum length $l_B = e^2/\epsilon k_BT$. For example, the Bjerrum length is about 7 Å in water at room-temperature 298 K. In our simulations, the value of the Bjerrum length l_B was varied between 1σ and 15σ. The system electroneutrality was maintained by adding monomer-like counterions to compensate for each charge on the polyelectrolyte chain. All charged particles in our simulations were monovalent ions with valence $q_i = \pm 1$.

In addition to electrostatic interactions, both charged and uncharged particles in the system interacted through the truncated-shifted Lennard-Jones potential,[50]

$$U_{\mathrm{LJ}}(r_{ij}) = \begin{cases} 4\epsilon_{\mathrm{LJ}}\left[\left(\frac{\sigma}{r_{ij}}\right)^{12} - \left(\frac{\sigma}{r_{ij}}\right)^{6} - \left(\frac{\sigma}{r_{\mathrm{cut}}}\right)^{12} + \left(\frac{\sigma}{r_{\mathrm{cut}}}\right)^{6}\right] & r \le r_{\mathrm{cut}}, \\ 0 & r > r_{\mathrm{cut}} \end{cases} \tag{36}$$

where r_{ij} is the distance between two interacting ith and jth beads, σ is the particle diameter that is chosen to be the same regardless of the type of particles, and r_{cut} is a cutoff distance beyond which the interaction potential is zero. The cutoff distance r_{cut} was equal to 2.5σ for polymer−polymer, and $2^{1/6}\sigma$ for polymer−counterion and counterion−counterion interactions. The value of the Lennard-Jones interaction parameter was varied between $\epsilon_{\mathrm{LJ}} = 0.1\ k_BT$ and $\epsilon_{\mathrm{LJ}} = 1.5\ k_BT$ for polymer−polymer interactions. The value of this parameter for polymer−counterion and counterion−counterion interactions was set to $\epsilon_{\mathrm{LJ}} = k_BT$. Note that the value of the interaction parameter $\epsilon_{\mathrm{LJ}} = 0.35\ k_BT$ between monomers corresponds to θ conditions for neutral polymers.

Simulations were carried out in a constant number of particles, constant volume, and constant temperature (NVT) ensemble with periodic boundary conditions. In our simulations, the simulation box size was varied between $L = 107.4\sigma$ and $L = 144.9\sigma$ depending on chain degree of polymerization to keep the monomer concentration constant and equal to $c = 10^{-4}\ \sigma^{-3}$. The electrostatic interactions in our simulations were calculated by the Particle−Particle Particle−Mesh (P^3M) method[18,50] implemented in LAMMPS,[51] which takes into account electrostatic interactions with all periodic images of the system.

The constant temperature was maintained by coupling the system to the Langevin thermostat. In this case, the motion of beads in the system is described by the following equation,

$$m\frac{d\vec{v}_i}{dt}(t) = \vec{F}_i(t) - \xi\vec{v}_i(t) + \vec{F}_i^R(t) \tag{37}$$

where m is the particle mass, $\vec{v}_i$ is the particle velocity, and $\vec{F}_i$ denotes the net deterministic force acting on the ith particle. The stochastic force $\vec{F}_i^R$ has a zero average value $\langle\vec{F}_i^R(t)\rangle = 0$

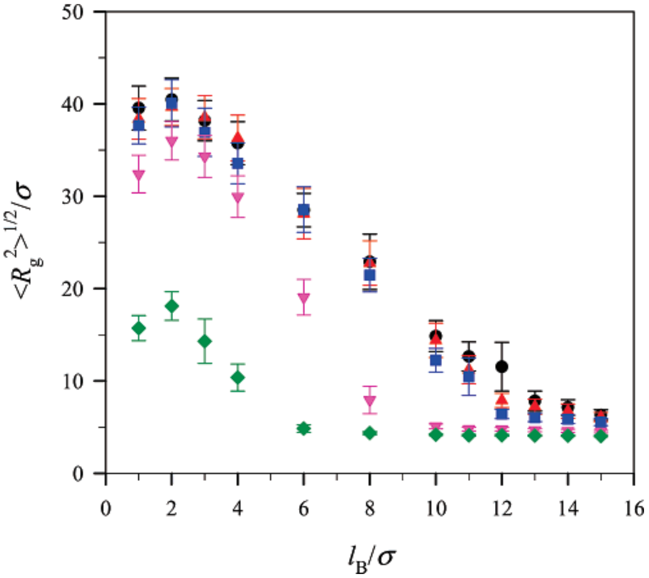

Figure 4. Dependence of the chain size on the value of the Bjerrum length for polyelectrolyte chain with the degree of polymerization $N = 304$, the fraction of charged monomers $f = ^1/_3$ for different values of the Lennard-Jones interaction parameters $\epsilon_{LJ} = 0.1\ k_BT$ (filled circles), $\epsilon_{LJ} = 0.3\ k_BT$ (filled triangles), $\epsilon_{LJ} = 0.5\ k_BT$ (filled squares), $\epsilon_{LJ} = k_BT$ (inverted filled triangles), and $\epsilon_{LJ} = 1.5\ k_BT$ (filled rhombs).

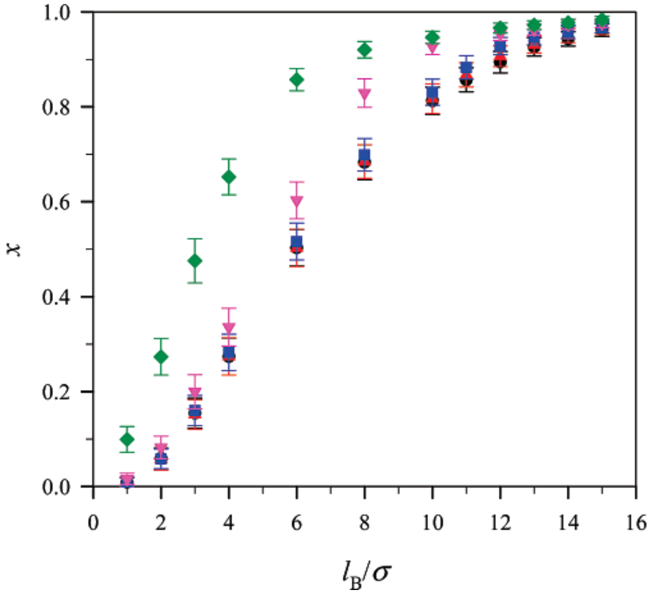

Figure 5. Dependence of the fraction of condensed counterions x on the value of the Bjerrum length for polyelectrolyte chain with the degree of polymerization $N = 304$, the fraction of charged monomers $f = ^1/_3$ for different values of the Lennard-Jones interaction parameters $\epsilon_{LJ} = 0.1\ k_BT$ (filled circles), $\epsilon_{LJ} = 0.3\ k_BT$ (filled triangles), $\epsilon_{LJ} = 0.5\ k_BT$ (filled squares), $\epsilon_{LJ} = k_BT$ (inverted filled triangles), and $\epsilon_{LJ} = 1.5\ k_BT$ (filled rhombs).

and δ functional correlations $\langle \vec{F}_i^R(t)\vec{F}_i^R(t')\rangle = 6\ k_BT\xi\delta(t - t')$. The friction coefficient ξ was set to $\xi = m/\tau_{LJ}$, where τ_{LJ} is the standard LJ time $\tau_{LJ} = \sigma(m/k_BT)^{1/2}$. The velocity-Verlet algorithm with a time step $\Delta t = 0.01\tau_{LJ}$ was used for integration of the equations of motion (eq 37).

Simulations were performed by using the following procedure: At the beginning of each simulation run, a negatively charged polyelectrolyte chain in self-avoiding walk configuration was placed in the center of the simulation box together with its counterions. The system was pre-equilibrated for 10^6 MD steps. This was followed by the production run lasting 3×10^6 MD steps. During the production run, we averaged the distribution functions of the number of monomers in beads and strings, the distribution function of the number of beads per chain, the chain radius of gyration, and fraction of condensed counterions.

3.2. Simulation Results. Dependence of the chain radius of gyration on the value of the Bjerrum length l_B and the value of the Lennard-Jones interaction parameter ϵ_{LJ} is shown in Figure 4. For all values of the Lennard-Jones interaction parameter ϵ_{LJ}, the chain size varies nonmonotonically with the value of the Bjerrum length. It first increases with the Bjerrum length (for the Bjerrum length values smaller than or equal to 2σ) then begins to decrease. The variation in the chain size with the value of the Bjerrum length is the manifestation of the two different mechanisms that are responsible for the chain conformational transformations and are controlled by the strength of the electrostatic interactions. The first mechanism that drives chain elongation is the intrachain electrostatic repulsion between charged monomers. With increasing the value of the Bjerrum length l_B, the electrostatic repulsion between charged monomers increases and forces a polyelectrolyte chain to adopt a more elongated (stretched) configuration. The second mechanism is the counterion condensation on the polymer backbone. As the value of the Bjerrum length increases, the electrostatic attraction of a counterion to a polymer backbone increases as well, resulting in a larger amount of counterions residing in the vicinity of the polymer backbone. These counterions reduce the effective charge on a polyelectrolyte chain weakening the intrachain electrostatic repulsion and leading to a decrease in chain size. However, this is only the initial stage of the counterion condensation process. With increasing of the number of condensed counterions on the polymer backbone, the electrostatic interactions between condensed counterions and charged monomers could lead to a local chain collapse.

This qualitative picture of the counterion condensation effect on the chain conformations is supported by Figure 5, which shows the dependence of the fraction of the condensed counterions x on the value of the Bjerrum length l_B. To obtain the fraction of the condensed counterions for this plot, we have surrounded each monomer by a sphere of radius $r_c = 1.5\sigma$ and counted all counterions with the center of mass within this cutoff distance from a monomer. The final list of the condensed counterions was examined for multiple entries such that each condensed counterion was counted only once. The fraction of condensed counterions increases with increasing of the value of the Bjerrum length. At small values of the Bjerrum length, $l_B < 3\sigma$, more than 80% of counterions leave a polyelectrolyte chain. In this interval of the Bjerrum lengths, the counterion configurational entropy loss due to its localization near the polymer backbone is much larger than the electrostatic attraction of a counterion to a polyelectrolyte chain. With increasing of the value of the Bjerrum length, the fraction of the condensed counterions increases and reaches about 30% at the value of the Bjerrum length $l_B \sim 4\sigma$ (for $\epsilon_{LJ} < 1.5\ k_BT$). At this value of the Bjerrum length, the configurational entropy loss is of the order of the electrostatic energy gain due to counterion condensation. For the largest value of the Bjerrum length, $l_B = 15\sigma$, more than 95% of counterions is condensed on the polymer backbone. For this value of the Bjerrum length, the electrostatic contribution to the counterion free energy is much larger than its configurational entropy part. The faster increase of the fraction of the condensed counterions x seen for polyelectrolytes in poor solvent conditions for the polymer backbone with $\epsilon_{LJ} = 1.5\ k_BT$ is due to the stronger chain collapse, resulting in the lower value of the local electrostatic potential and stronger attraction of a counterion to a polymer chain.

Table 2. Typical Conformations of Polyelectrolyte Chain with Degree of Polymerization $N = 304$ and Fraction of Charged Monomers $f = {}^1/_3$

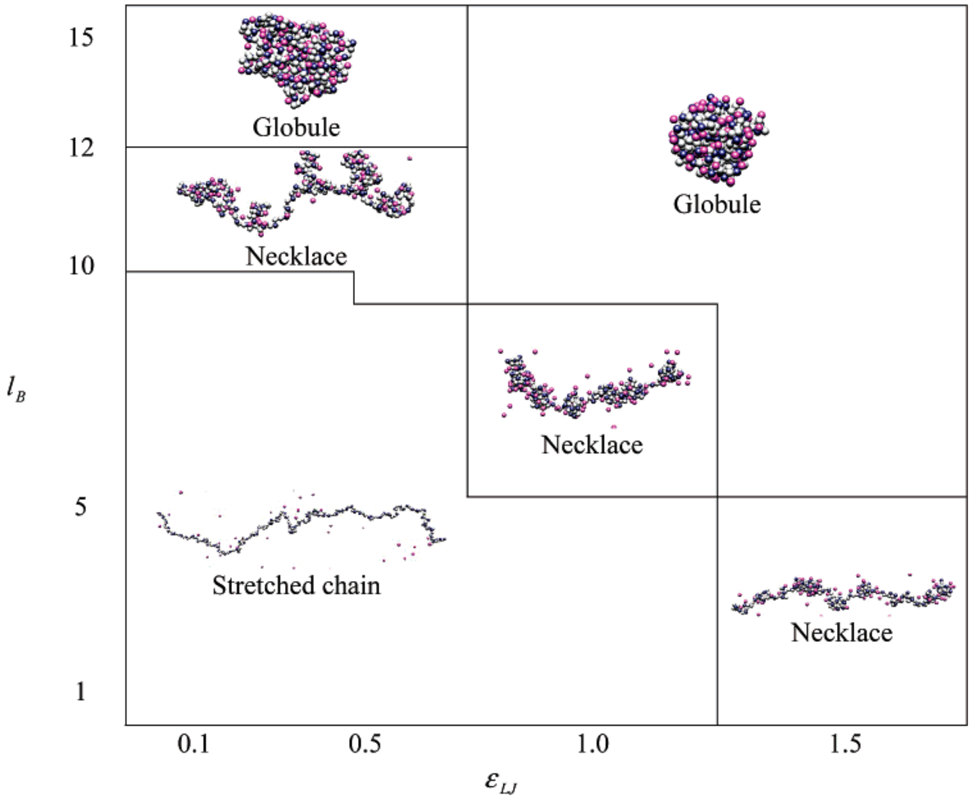

Table 2 shows typical chain conformations in the $\epsilon_{LJ}-l_B$ plane. At small values of the Lennard-Jones interaction parameter $\epsilon_{LJ} < k_BT$, which corresponds to the interval of good and weak poor solvent conditions for the polymer backbone, a polyelectrolyte chain undergoes stretched chain−necklace−globule conformational transformations with increasing of the value of the Bjerrum length. This cascade of transformations is a result of counterion condensation on the polymer backbone. Note that the different chain conformations shown in Table 2 are qualitatively similar to those obtained by Limbach el al.[30] in their simulations of a polyelectrolyte chain. To quantify the effect of counterions on the chain conformations, we will consider separately different conformation regimes.

We will first analyze chain behavior in the stretched chain regime. In this interval of the Bjerrum lengths, the condensed counterions mainly contribute to the reduction of the net polymeric charge, weakening intrachain electrostatic repulsion. The chain size R_e in this regime can be estimated by balancing the chain conformational free energy $k_BTR_e^2/b^2N$ and electrostatic repulsion between ΔfN uncompensated charges on the polymer backbone, $k_BT\, l_B(\Delta fN)^2/R_e$.[3] Thus, the chain size scales with the fraction of condensed counterions and the interaction parameter u as

$$R_e \approx bu^{1/3}(1 - x)^{2/3}f^{2/3}N \approx bu^{1/3}\Delta f^{2/3}N \qquad (38)$$

Figure 6 shows dependence of the reduced chain size $\Delta f^{1/3}R_e/u^{1/3}$ on the polyelectrolyte valence ΔfN for the different values of the Bjerrum length and the Lennard-Jones interaction parameter ϵ_{LJ}. As one can see, the data points for the large values of the Bjerrum length $l_B > 2\sigma$ collapsed into one universal line with slope one, indicating that the solvent quality has almost no effect on the chain conformations. Note that, in this regime, a polyelectrolyte chain can be viewed as an array of the electrostatic blobs with size $D_e \approx bu^{-1/3}\Delta f^{-2/3}$ containing $g_e \approx u^{-2/3}\Delta f^{-4/3}$ monomers.[3,49] The chain conformations inside an electrostatic blob will remain unperturbed by short-range monomer−monomer interactions as long as the number of monomers in the electrostatic blob is smaller than $g_e < |\tau|^{-2}$. This is indeed the case for the values of the Lennard-Jones interaction parameter $0.1\ k_BT \leq \epsilon_{LJ} \leq 0.5\ k_BT$. For the value of the Lennard-Jones interaction parameter $\epsilon_{LJ} = k_BT$, the monomer−

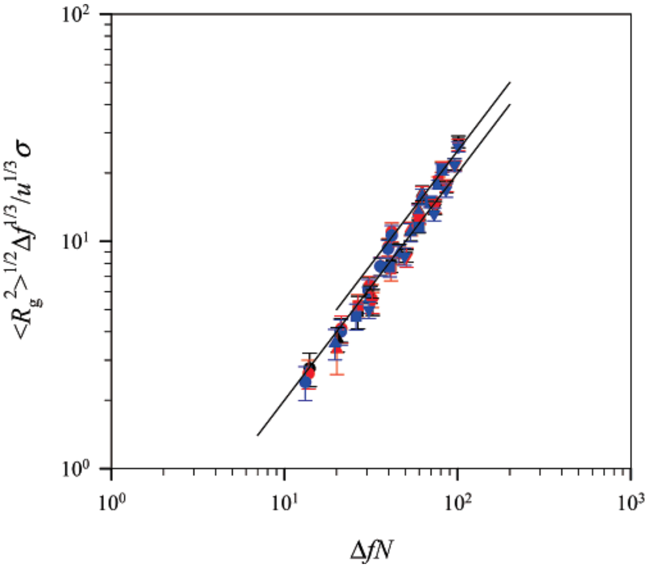

Figure 6. Universal plot of the reduced chain size on the chain valence ΔfN for chains with degrees of polymerizations $N = 124$ (filled circles), $N = 187$ (filled triangles), $N = 244$ (filled squares), and $N = 304$ (inverted filled triangles) for different values of the Lennard-Jones interaction parameters $\epsilon_{LJ} = 0.1\ k_BT$ (black symbols), $\epsilon_{LJ} = 0.3\ k_BT$ (red symbols), and $\epsilon_{LJ} = 0.5\ k_BT$ (blue symbols). The solid lines have slope one.

monomer interactions start to perturb chain conformations inside an electrostatic blob, resulting in additional chain shrinkage (see also Figure 4). This value of the Lennard-Jones interaction parameter corresponds to true poor solvent conditions for the polymer backbone. It is important to point out that the data points corresponding to the values of the Bjerrum length $l_B = 1\sigma$ and 2σ deviates from this universal line, indicating that condensed counterions can slightly perturb chain conformations even in the stretched chain regime.

Condensed counterions lead to a complete chain collapse for the values of the Bjerrum length $l_B \geq 12\sigma$. The chain collapse in this regime is caused by the correlation-induced attraction between the condensed counterion and the weakly fluctuating charge background of the collapsed polyelectrolyte chain. The polymeric density inside a globule is stabilized by three-body monomer−monomer repulsion. The globular size in this regime is estimated as

$$R_{\rm glob} \approx (N/\rho)^{1/3} \approx bu^{-1/5}(xf)^{-4/15}N^{1/3} \qquad (39)$$

In the derivation of the eq 39, we used the expression for the polymer density ρ from the Table 1 for the three-body SC regime. The stability of the polymeric globule is insured by the dominance of the globular surface energy, $k_BT\gamma R_{\rm glob}{}^2/b^2$, over the intrachain electrostatic repulsion between uncompensated charges, $k_BTl_B(\Delta fN)^2/R_{\rm glob}$. Both terms become of the same order in magnitude when

$$N \approx \frac{x}{(1-x)^2 f} \approx \frac{xf}{\Delta f^2} \qquad (40)$$

Equation 40 determines the boundary of the globule regime as a function of the fraction of the condensed counterions and the chain's degree of polymerization, N. Note that this equation is an analog of the Rayleigh stability condition for the charged polymeric globule.

The dependence of the reduced square root of the mean-square radius of gyration, $\langle R_g^2\rangle^{1/2}/R_{\rm glob}$, of chains with the degree of polymerizations $N = 124-304$ on the reduced value of the total charge valence, $\Delta fN/(xfN)^{1/2}$, of the globule is plotted in Figure 7. As expected, all data points collapse into one universal plot. A spherical globule is stable when its net charge valence ΔfN is smaller than the square root of the charge valence of the condensed counterions $(xfN)^{1/2}$. When the globule valence ΔfN is larger than 0.48 $(xfN)^{1/2}$, a spherical globule becomes unstable. As the fraction of the condensed counterions decreases further, a polymer chain adopts necklace-like conformation of dense beads connected by strings. This transformation is triggered by the decrease in the value of the Bjerrum length l_B. The values of the Lennard-Jones interaction parameter in this regime correspond to either positive or weakly negative values of the second-virial coefficient for the monomer−monomer interactions. In this range of the Lennard-Jones interaction parameter, the necklace structure is strongly fluctuating, resulting in very broad distribution in the number of monomers in a bead and in a string. The necklace formation and chain collapse in this interval of parameters can be exclusively attributed to the counterion condensation. It is also important to point out that the equilibrium density inside the collapsed chain or collapsed sections of the chain is stabilized by three-body monomer−monomer repulsion.

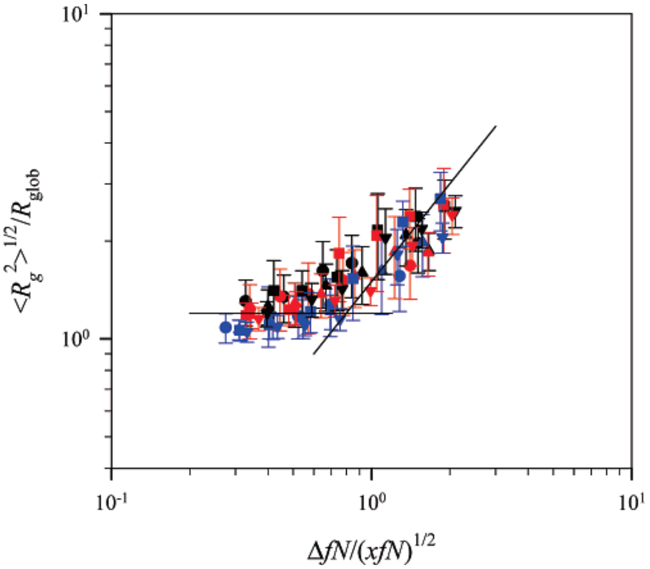

Figure 7. Reduced square-root mean-square radius of gyration $\langle R_g^2\rangle^{1/2}/R_{\rm glob}$ as a function of the reduced valence of charged globule, $\Delta fN/(xfN)^{1/2}$, for chains with degrees of polymerizations $N = 124$ (filled circles), $N = 187$ (filled triangles), $N = 244$ (filled squares), and $N = 304$ (inverted filled triangles) for different values of the Lennard-Jones interaction parameters $\epsilon_{\rm LJ} = 0.1\ k_BT$ (black symbols), $\epsilon_{\rm LJ} = 0.3\ k_BT$ (red symbols), and $\epsilon_{\rm LJ} = 0.5\ k_BT$ (blue symbols).

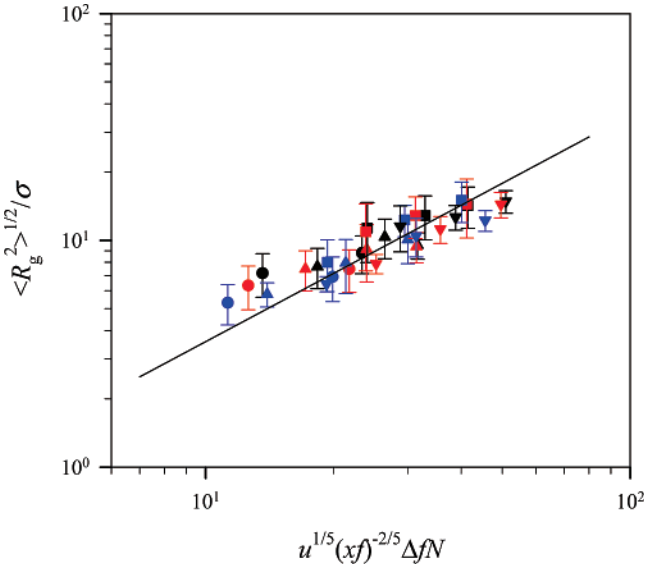

Figure 8. Square-root mean-square radius of gyration as a function of the parameter $u^{1/5}(xf)^{-2/5}\Delta fN$ for chains with degrees of polymerizations $N = 124$ (filled circles), $N = 187$ (filled triangles), $N = 244$ (filled squares), and $N = 304$ (inverted filled triangles) for different values of the Lennard-Jones interaction parameters $\epsilon_{\rm LJ} = 0.1\ k_BT$ (black symbols), $\epsilon_{\rm LJ} = 0.3\ k_BT$ (red symbols), and $\epsilon_{\rm LJ} = 0.5\ k_BT$ (blue symbols). The solid line has slope one.

In the interval of the Bjerrum lengths $10\sigma \leq l_B \leq 12\sigma$, a correlation-induced attraction between condensed counterions results in local chain collapse and formation of the necklace globule. The size of the necklace globule is proportional to the chain's uncompensated charge ΔfN (see Table 1) and it increases with increasing the charge imbalance, ΔfN. To test this relation in Figure 8, we have plotted the dependence of the chain size versus scaling model prediction for the value of

$$R_e \approx u^{1/5}(xf)^{-2/5}(1-x)fN \approx u^{1/5}(xf)^{-2/5}\Delta fN \qquad (41)$$

As one can see, the agreement between the results of the computer simulations and a scaling model is good. This also explains why we have a reasonably good collapse of the data in the interval $\Delta fN > 0.48\,(xfN)^{1/2}$. By comparing eqs 39 and 41, one can establish that eq 41 can be rewritten as

$$R_e \approx u^{2/5}(xf)^{11/30}N^{1/6}R_{\mathrm{glob}}\Delta fN/(xfN)^{1/2} \qquad (42)$$

Thus, the ratio of R_e/R_{glob} is proportional to $\Delta fN/(xfN)^{1/2}$. The proportionality coefficient has weak dependence on the value of the Bjerrum length and chain degree of polymerization in the range of parameters used in our simulations.

Equations 18 and 33 give simple relations between the optimal number of monomers in a bead, m_b^*, and the fraction of condensed counterions, x. We tested these relations for polyelectrolyte chains with different strength of the electrostatic interactions and value of the Lennard-Jones interaction parameter $\epsilon_{LJ} = 1.5\ k_BT$ (see Figure 9). To improve statistics, each point is averaged over all beads with the number of monomers, m_b, within five monomers of the most probable (optimal) number of monomers in bead ($m_b^* - 5 \le m_b \le m_b^* + 5$). The optimal number of monomers in a bead, m_b^*, was obtained by fitting the bead distribution function to the distribution function derived by Liao et al.[26] The growth of beads with increasing the Bjerrum length is an indication of the counterion condensation. The energy gain due to counterion localization inside and around beads increases with the increasing of the value of the Bjerrum length. In our simulation, the average concentration of the counterion was kept constant. Thus, the entropy loss due to counterion localization was unchanged.

In the case of the very poor solvent conditions for the polymer backbone, $\epsilon_{LJ} = 1.5\ k_BT$, a polyelectrolyte chain forms a necklace globule already at the lowest values of the Bjerrum length $l_B < 3\sigma$. The necklace formation in this range of the parameters is a result of the optimization of the favorable short-range monomer−monomer attraction and electrostatic repulsion between uncompensated charges. To show that this is indeed the case, in Figure 9a, we have plotted the dependence of the parameter um_b^* on the fraction of the condensed counterions, x. As one can see, all data points for different chains' degrees of polymerizations and different values of the Bjerrum length, $l_B = 1\sigma$ and 2σ, have collapsed into one universal plot. Note that the data points are close to the ones obtained in simulations of the polyelectrolyte chains in poor solvent conditions for the polymer backbone in salt solutions (see open symbols).[41] The solid line in this plot corresponds to eq 33.

The different functional dependence is seen in Figure 9b, which shows the dependence of the number of monomers in the optimal bead m_b^* on the fraction of the condensed counterions x for the values of the Bjerrum length, $l_B = 3\sigma$ and 4σ. We have also added to this plot the data points from simulations of salt-free solutions by Liao et al.[26] and data points from simulations with added salt by Jeon and Dobrynin.[41] The different data sets are close to the universal curve corresponding to eq 18. Thus, parts a and b of Figure 9 provide further evidence for the existence of two different mechanisms responsible for the bead formation.

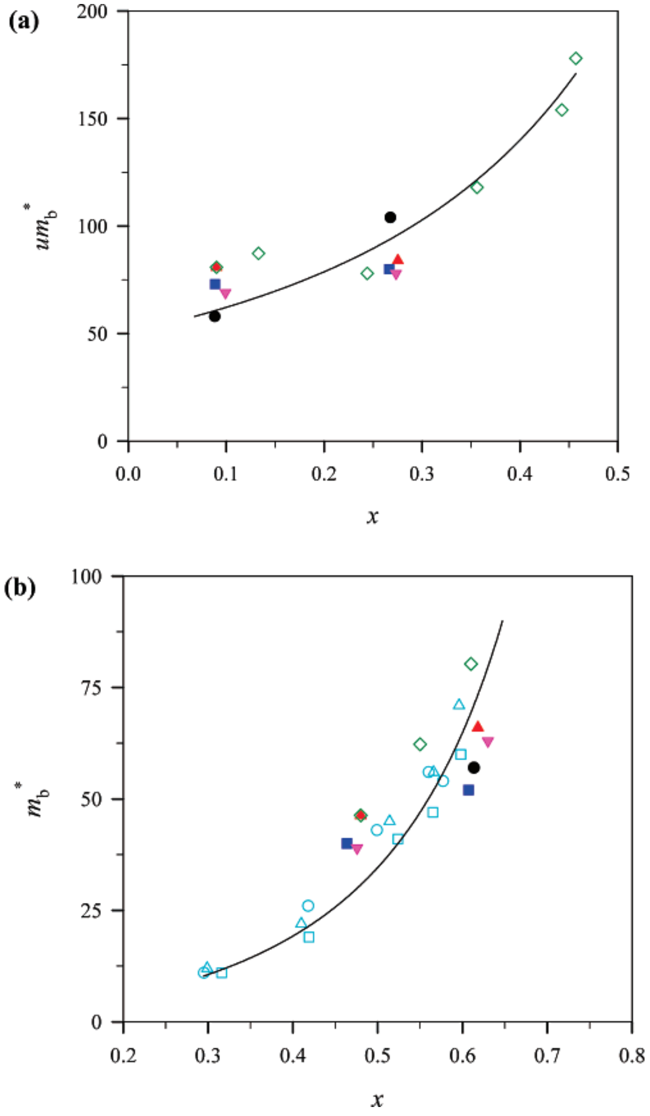

Figure 9. Dependence of the optimal number of monomers in a bead m_b^* on the fraction of the condensed counterions for chains with different degrees of polymerization N. (a) $\epsilon_{LJ} = 1.5\ k_BT$, $l_B = 1\sigma$ and 2σ, for the chains with the degrees of polymerization $N = 124$ (filled circles), $N = 187$ (filled triangles), $N = 244$ (filled squares), and $N = 304$ (inverted filled triangles). The solid line is given by the equation $um_b^* = 50.4/(1 - x)^2$. Open symbols show data points from ref 41 $N = 187$ (rhombs). (b) $\epsilon_{LJ} = 1.5\ k_BT$, $l_B = 3\sigma$ and 4σ, for the chains with the degrees of polymerizations $N = 124$ (filled circles), $N = 187$ (filled triangles), $N = 244$ (filled squares), and $N = 304$ (inverted filled triangles). The solid line is given by the equation $m_b^* = 17.3x/(1 - x)^2$. Open symbols show data points from ref 41 $N = 187$ (rhombs) and from ref 26 $N = 187$ (circles), $N = 244$ (triangles), and $N = 373$ (squares).

4. Conclusions

We have presented a necklace model of a polyelectrolyte chain in which the necklace structure is produced by the correlation-induced attractive interactions between condensed counterions and charged monomers. Because of these interactions, the necklace structure can even be formed in the good solvent conditions for the polymer backbone. The transition to the necklace globule depends on both the value of the Bjerrum length determining the strength of the electrostatic interactions and the value of the Lennard-Jones interaction parameter, which controls the solvent quality for the polymer backbone. According to this model, the parameters of the necklace such as number of monomers in a bead, bead size, number of beads per chain, and string length connecting the neighboring beads show strong dependence on the value of the Bjerrum length. In particular, in the counterion-correlation regime, the beads of the necklace globule grow in size with increasing the value of the Bjerrum length. By using this new necklace model, we have calculated the diagram of state of a polyelectrolyte chains as a function of the fraction of the condensed counterions and net charge of a polyelectrolyte chain (see Figure 3).

To test the predictions of the necklace model, we have performed molecular dynamics simulations of a polyelectrolyte chain with the degrees of polymerization $N = 124-304$ and fraction of the charged monomers $f = {}^1/_3$. In these simulations, we have varied the value of the Bjerrum length l_B between 1σ and 15σ and the value of the Lennard-Jones interaction parameter ϵ_{LJ} between 0.1 k_BT and 1.5 k_BT. This interval of the Lennard-Jones interaction parameter covers the good and poor solvent regimes for the polymer backbone. Our simulations confirmed the predictions of the scaling model that formation of the necklace globule is possible even in the good solvent conditions, $\epsilon_{LJ} = 0.1$ k_BT. In this range of parameters, the Rayleigh stability condition of a spherical globule with condensed counterions depends on the ratio of the net globular charge ΔfN to the square root of the net charge carried by condensed counterions, $(xfN)^{1/2}$ (see Figure 7). It is completely different from the case of a charged globule formed in poor solvent conditions for the polymer backbone. For all studied systems, the chain size shows nonmonotonic dependence on the value of the Bjerrum length. It first increases with increasing of the value of the Bjerrum length and then starts to decrease. The location of the maximum on the chain size−Bjerrum length curve depends on the solvent quality for the polymer backbone (value of the Lennard-Jones interaction parameter ϵ_{LJ}). For the larger values of the interaction parameter ϵ_{LJ}, a chain forms a collapsed spherical globule for smaller values of the Bjerrum length. This indicates that short-range monomer−monomer interactions still play an important role in determining the chain configuration (see Figure 4).

The model of the counterion-correlation induced chain collapse can be extended to the case of the semiflexible polyelectrolytes.[20] Semiflexible polymers in poor solvent conditions for the polymer backbone form torroidal globule. A charged semiflexible polyelectrolyte chain adopts rings on a string conformation of collapsed torroidal globules connected by the stretched strings of monomers.[52−58] This structure optimizes the short-range monomer−monomer attractive interactions, the chain's bending energy, and long-range electrostatic repulsion between charged groups. The increase of the Bjerrum length in this case will also trigger the counterion condensation on the torroidal globules, leading to correlation-induced attraction between condensed counterions and charged monomers and promoting further chain collapse. In this case, one should expect a collapse of a semiflexible polyelectrolyte chain by condensed counterion even in a good solvent condition for the polymer backbone. Note that the strength of the electrostatic interactions between a counterion and a polyelectrolyte chain can be varied by changing the counterion valence. It is interesting to point out that the condensation of the multivalent ions on the semiflexible polyelectrolyte chain models the DNA condensation by multivalent counterions.[44,45] We are planning to address these questions in our future publications.

Acknowledgment. We are grateful to the donors of the American Chemical Society Petroleum Research Fund for support of this research under the grant PRF 44861-AC7.

References and Notes

(1) Hara, M. *Polyelectrolytes*; Marcel Dekker: New York, 1993.
(2) Barrat, J. L.; Joanny, J. F. *Adv. Chem. Phys.* **1996**, *94*, 1.
(3) Dobrynin, A. V.; Rubinstein, M. *Prog. Polym. Sci.* **2005**, *30*, 1049.
(4) Forster, S.; Schmidt, M. *Adv. Polym. Sci.* **1995**, *120*, 51.
(5) Holm, C.; Joanny, J. F.; Kremer, K.; Netz, R. R.; Reineker, P.; Seidel, C.; Vilgis, T. A.; Winkler, R. G. *Adv. Polym. Sci.* **2004**, *166*, 67.
(6) Manning, G. S. *J. Chem. Phys.* **1969**, *51*, 924.
(7) Manning, G. S. *Physica A* **1996**, *231*, 236.
(8) Manning, G. S. *Ber. Bunsen-Ges. Phys. Chem.* **1996**, *100*, 909.
(9) Oosawa, F. *Polyelectrolytes*; Marcel Dekker: New York, 1971.
(10) Raphael, E.; Joanny, J. F. *Europhys. Lett.* **1990**, *13*, 623.
(11) Schiessel, H.; Pincus, P. *Macromolecules* **1998**, *31*, 7953.
(12) Schiessel, H. *Macromolecules* **1999**, *32*, 5673.
(13) Winkler, R. G.; Gold, M.; Reineker, P. *Phys. Rev. Lett.* **1998**, *80*, 3731.
(14) Gonzalez-Mozuelos, P.; Delacruz, M. O. *J. Chem. Phys.* **1995**, *103*, 3145.
(15) Castelnovo, M.; Sens, P.; Joanny, J. F. *Eur. Phys. J. E* **2000**, *1*, 115.
(16) Brilliantov, N. V.; Kuznetsov, D. V.; Klein, R. *Phys. Rev. Lett.* **1998**, *81*, 1433.
(17) Dobrynin, A. V.; Rubinstein, M. *Macromolecules* **2001**, *34*, 1964.
(18) Dobrynin, A. V. Molecular simulations of charged polymers. In *Simulation Methods for Polymers*; Kotelyanskii, M., Theodorou, D. N., Eds.; Marcel Dekker: New York, 2004.
(19) Dobrynin, A. V.; Rubinstein, M. *Macromolecules* **1999**, *32*, 915.
(20) Ghosh, K.; Carri, G. A.; Muthukumar, M. *J. Chem. Phys.* **2001**, *115*, 4367.
(21) Liao, Q.; Dobrynin, A. V.; Rubinstein, M. *Macromolecules* **2003**, *36*, 3386.
(22) Liao, Q.; Dobrynin, A. V.; Rubinstein, M. *Macromolecules* **2003**, *36*, 3399.
(23) Muthukumar, M. *J. Chem. Phys.* **2004**, *120*, 9343.
(24) Khokhlov, A. R. *J. Phys. A: Math. Gen.* **1980**, *13*, 979.
(25) Dobrynin, A. V.; Rubinstein, M.; Obukhov, S. P. *Macromolecules* **1996**, *29*, 2974.
(26) Liao, Q.; Dobrynin, A. V.; Rubinstein, M. *Macromolecules* **2006**, *39*, 1920.
(27) Limbach, H. J.; Holm, C. *J. Chem. Phys.* **2001**, *114*, 9674.
(28) Limbach, H. J.; Holm, C.; Kremer, K. *Europhys. Lett.* **2002**, *60*, 566.
(29) Limbach, H. J.; Holm, C. *Comput. Phys. Commun.* **2002**, *147*, 321.
(30) Limbach, H. J.; Holm, C. *J. Phys. Chem. B* **2003**, *107*, 8041.
(31) Limbach, H. J.; Holm, C.; Kremer, K. *Macromol. Symp.* **2004**, *211*, 43.
(32) Lyulin, A. V.; Dunweg, B.; Borisov, O. V.; Darinskii, A. A. *Macromolecules* **1999**, *32*, 3264.
(33) Micka, U.; Holm, C.; Kremer, K. *Langmuir* **1999**, *15*, 4033.
(34) Micka, U.; Kremer, K. *Europhys. Lett.* **2000**, *49*, 189.
(35) Migliorini, G.; Lee, N.; Rostiashvili, V.; Vilgis, T. A. *Eur. Phys. J. E* **2001**, *6*, 259.
(36) Morawetz, H. *J. Polym. Sci., Part B: Polym. Phys.* **2002**, *40*, 1080.
(37) Solis, F. J.; de la Cruz, M. O. *Macromolecules* **1998**, *31*, 5502.
(38) Kiriy, A.; Gorodyska, G.; Minko, S.; Jaeger, W.; Stepanek, P.; Stamm, M. *J. Am. Chem. Soc.* **2002**, *124*, 13454.
(39) Aseyev, V. O.; Klenin, S. I.; Tenhu, H. *J. Polym. Sci., Part B: Polym. Phys.* **1998**, *36*, 1107.
(40) Baigl, D.; Sferrazza, M.; Williams, C. E. *Europhys. Lett.* **2003**, *62*, 110.
(41) Jeon, J.; Dobrynin, A. V. *J. Phys. Chem. B* **2006**, *110*, 24652.
(42) Kramarenko, E. Y.; Khokhlov, A. R.; Yoshikawa, K. *Macromolecules* **1997**, *30*, 3383.
(43) Kramarenko, E. Y.; Khokhlov, A. R.; Yoshikawa, K. *Macromol. Theory Simul.* **2000**, *9*, 249.
(44) Grosberg, A. Y.; Nguyen, T. T.; Shklovskii, B. I. *Rev. Mod. Phys.* **2002**, *74*, 329.
(45) Levin, Y. *Rep. Prog. Phys.* **2002**, *65*, 1577.
(46) Grosberg, A. Y.; Khokhlov, A. R. *Statistical Physics of Macromolecules*; American Institute of Physics: New York, 1994.
(47) de Gennes, P. G. *Scaling Concepts in Polymer Physics*; Cornell University Press: Ithaca, NY, 1979.
(48) Rubinstein, M.; Colby, R. H. *Polymer Physics*; Oxford University Press: New York, 2003.
(49) Dobrynin, A. V.; Colby, R. H.; Rubinstein, M. *Macromolecules* **1995**, *28*, 1859.
(50) Frenkel, D.; Smit, B. *Understanding Molecular Simulations*; Academic Press: San Diego, 2001.
(51) Plimpton, S. *LAMMPS User's Manual*; Sandia National Laboratory: Albuquerque, NM, 2005.
(52) Iwaki, T. *J. Chem. Phys.* **2006**, *125*, 224901.
(53) Sakaue, T.; Yoshikawa, K. *J. Chem. Phys.* **2006**, *125*, 074904.
(54) Yoshikawa, K.; Yoshinaga, N. *J. Phys. Condens. Matter* **2005**, *17*, S2817.
(55) Miyazawa, N.; Sakaue, T.; Yoshikawa, K.; Zana, R. *J. Chem. Phys.* **2005**, *122*, 044902.
(56) Iwaki, T.; Yoshikawa, K. *Europhys. Lett.* **2004**, *68*, 113.
(57) Hayashi, Y. *Europhys. Lett.* **2004**, *68*, 536.
(58) Sakaue, T. *J. Chem. Phys.* **2004**, *120*, 6299.

MA071005K